IEEE Access
Multidisciplinary | Rapid Review | Open Access Journal

Date of publication xxxx 00, 0000, date of current version xxxx 00, 0000.

Digital Object Identifier 10.1109/ACCESS.2023.0322000

LGAG-Net: Lesion-Guided Adaptive Graph Network for Bone Abnormality Detection from Musculoskeletal Radiograph

YONG LIAO[1,2], XIANG LI[1,2], and CHENGFENG PENG[1,2]

[1]Application of non-linear Functional Theory Drives the Transformation of Scientific and Technological Innovation Teams in Ordinary Universities in Hunan province, Xiangnan University, Chenzhou, 423000, China
[2]Microelectronics and Optoelectronics Technology Key Laboratory of Hunan Higher Education, School of Physics and Electronic Electrical Engineering, Xiangnan University, Chenzhou, 423000, China

Corresponding author: CHENGFENG PENG (e-mail: pchfeng0309@gmail.com).

This work was supported in part by the Natural Science Foundation of Hunan Province(No.2023JJ50066), the Chenzhou Science and Technology Development Plan Project (No.ZDYF2020161), the Scientific Research Fund of Hunan Provincial Education Department (No:22B0812), in part by the 2021 Hunan Colleges and Universities Innovation and Entrepreneurship School-Enterprise Cooperation Base (No.74th), the Chenzhou Science and Technology Development Plan (No.ZDYF2020161), the Innovation and Entrepreneurship Education Center in Ordinary Universities in 2022(No.70th), the Chenzhou Low Carbon Intelligent Manufacturing Technology Research, the Applied Characteristic Disciplines of Electronic Science and Technology of Xiangnan University under Grant (No.XNXY20221210), Aid program for Science and Technology Innovative Research Team in Higher Educational Institutions of Hunan Province.

ABSTRACT Musculoskeletal abnormality is routinely presented in tissues and organs of the human locomotor system across the life course, and it is essential to detect musculoskeletal abnormality in X-rays. However, it is difficult to diagnose musculoskeletal abnormality from Radiographs due to the following issues: 1) There are other interfering organ tissues in the complicated backgrounds; 2)The MURA dataset contains seven different musculoskeletal radiographs, which makes general convolution neural networks unable to model the weird relationship between them. To address such problems, a Lesion-Guided Adaptive Graph Network (LGAG-Net) is proposed for bone abnormality detection from musculoskeletal radiograph, where the Lesion-guided Recurrent Feature Sampling (LRFS) module is first designed to localize the corresponding musculoskeletal abnormality regions, and then the Adaptive Graphsage Attention (AGA) module is developed to perform bone abnormality detection on the located musculoskeletal abnormality regions. Experiments on MURA dataset show that the proposed LGAG-Net can achieve an accuracy of 87.81% and Cohen Kappa statistic of 0.868, which outperforms the state-of-the-art methods, assisting the radiologists to rapidly estimate the physical development in patients.

INDEX TERMS Surface defect segmentation; multi-view learning; residual attention; Gaussian normalization

I. INTRODUCTION

Musculoskeletal complications are prevalent across the life course, and occur frequently with other non-communicable diseases in multimorbidity health states [1]–[3], about one-third to one-fifth of people suffer from musculoskeletal pain [4]. According to the statistics, the global burden of musculoskeletal diseases increases significantly between the years 2000 and 2015 [5], where over 50% of people aged 18 and above are affected by musculoskeletal diseases in the United States [6], and in China, musculoskeletal diseases are one of the three leading causes of disability [7].

Musculoskeletal conditions will result in great damage to the human locomotor system, affecting the comprised tissues and organs, such as muscles, bones, joints, ligaments, and tendons [8]. The fast development of digital imaging technologies in the medical domain provides basic tools for doctors to diagnose bone diseases and abnormalities in bones are routinely diagnosed manually by professional radiologists to analyze specific conditions based on radiographs. In the fight against bone diseases, timely abnormality detection is critical for further diagnosis and treatment. However, a large number of tasks and time-consuming process result in an overloaded workload for radiologists, and the situation is exacerbated for those in underdeveloped areas [9]. There is a pressing need for rapid and effective computer-aided detection (CAD) methods to identify abnormality in bones, and thereby decrease the

burden and error rates on radiologists.

Over the past decade, a number of research groups have focused on developing CAD tools to extract abnormal features associated with certain diseases from musculoskeletal X-Rays. [10] utilizes photogrammetry to detect thoracic musculoskeletal abnormalities in preterm infants. Vibrational spectroscopic techniques are applied to assess bone quality [11]. [12] detect the musculoskeletal abnormalities in children with mucopolysaccharidoses based on pediatric gait, arms, legs, and spine. In addition, a number of traditional image processing methods are proposed to detect bone fracture [13]–[15]. However, the accuracy of these CAD tools has not achieved a significantly high level of diagnosis for radiologists. There is an urgent need for an appropriate and accurate approach to implementing abnormality detection with high accuracy.

The machine learning, including support vector machines, Naive Bayes, K-nearest neighborhood (KNNs) and random forest, has also provided sound results in the field of medicine [16] [17]. The four different classifiers LBF SVM (Radial Basis Function support vector machine), linear SVM, Logistic Regression and Decision tree are used for abnormality detection in bones [18]. [19] propose a computer-assisted solution that combines canny edge with SVM Classifier for bone anomaly detection in X-Ray images. These machine learning approaches help radiologists diagnose musculoskeletal conditions much more accurately and overcome the disadvantages of traditional CAD tools previously mentioned, but most of them are poor in robustness because the picture quality and other factors are able to result in great variabilities in the algorithm recognition results.

Recently, deep learning has achieved superior performance in image recognition, classification, and segmentation, which has spurred application for abnormality detection in bones with deep learning. [20] investigates deep transfer learning to improve the performance in detecting abnormalities of upper extremities based on DenseNet-169, DenseNet-201, and InceptionResNetV2. [21] develop the ensemble200 model including DenseNet201, MobileNet, and NASNetMobile to improve the performance consistency and generalization of abnormality detection in musculoskeletal radiographs. [22] propose the GnCNNr model which utilizes group normalization, weight standardization, and cyclic learning rate scheduler to enhance the performance of the model for musculoskeletal abnormality detection. [23] introduces a novel tool to assist radiologists in automatically detecting abnormalities in musculoskeletal radiographs and leverages CAM to localize the abnormality in the image. A complicated capsule network architecture is introduced for musculoskeletal radiographs abnormality detection and it can vanquish the serious limitations of convolutional neural networks when the images are rotated and deformed [1]. [24] create an ensemble of 10 convolutional neural networks to identify and localizes fractures from the appearance of radiographs. A multi-network framework consisting of 2D-CNN and GCN is presented for the detection of automatic abnormalities in musculoskeletal radiographs [25].

Although these methods have shown good performance in musculoskeletal abnormality detection, it is still challenging because of the complexity of this task. First, there are a number of interfering organ tissues in the complicated backgrounds, as shown in Fig. 1 (a) and (b), where the abnormal regions are small while others are redundant for diagnosis. Second, the abnormal and normal elbows are always similar, leading to confusion regarding abnormality detection, as shown in Fig. 1 (c) and (d). Third, it is difficult for the convolutional neural networks to model the abnormal dependencies between different musculoskeletal radiographs, including the finger, humerus, elbow, forearm, hand, shoulder, and wrist, resulting in poor performance on musculoskeletal abnormality detection.

To address these problems, a Lesion-Guided Adaptive Graph Network (LGAG-Net) is proposed for bone abnormality detection, where the Lesion-guided Recurrent Feature Sampling (LRFS) module is first devised to focus on the musculoskeletal abnormality regions from musculoskeletal radiograph, and then the Adaptive Graphsage Attention (AGA) module is developed to diagnose bone abnormality on the musculoskeletal abnormality regions. The main contributions of this paper are summarized as follows.

(1) The Lesion-guided Recurrent Feature Sampling (LRFS) module is designed to capture the musculoskeletal abnormality regions, where the recurrent sampling strategy is proposed for obtaining the most representative features from the feature regions;
(2) The Adaptive Graphsage Attention (AGA) module is developed to diagnose bone abnormality in the abnormal bone regions, where the adaptive graph attention module can aggregate the information between adjacent nodes instead of learning the attention weights in every node.
(3) Experiments on the MURA dataset validate the effectiveness of the proposed LGAG-Net, and it can assist radiologists in rapidly estimating the physical development of patients.

The remainder of the paper is organized as follows: Section II describes the proposed LGAG-Net. Section III shows the experiments, while the conclusions are given in IV.

II. LESION-GUIDED ADAPTIVE GRAPH NETWORK FOR MUSCULOSKELETAL ABNORMALITIES DETECTION

In this section, a Lesion-Guided Adaptive Graph Network (LGAG-Net) is proposed for musculoskeletal abnormalities detection, as shown in Fig. 2, and it consists of two modules: Lesion-guided Recurrent Feature Sampling (LRFS) module and Adaptive Graphsage Attention (AGA) module, which are described as follows.

A. LESION-GUIDED RECURRENT FEATURE SAMPLING MODULE FOR ABNORMAL REGIONS LOCATION

Abnormality detection in musculoskeletal radiographs is routinely implemented to act on the finger, wrist, elbow, forearm, hand, shoulder, and humerus of the human skeletal system.

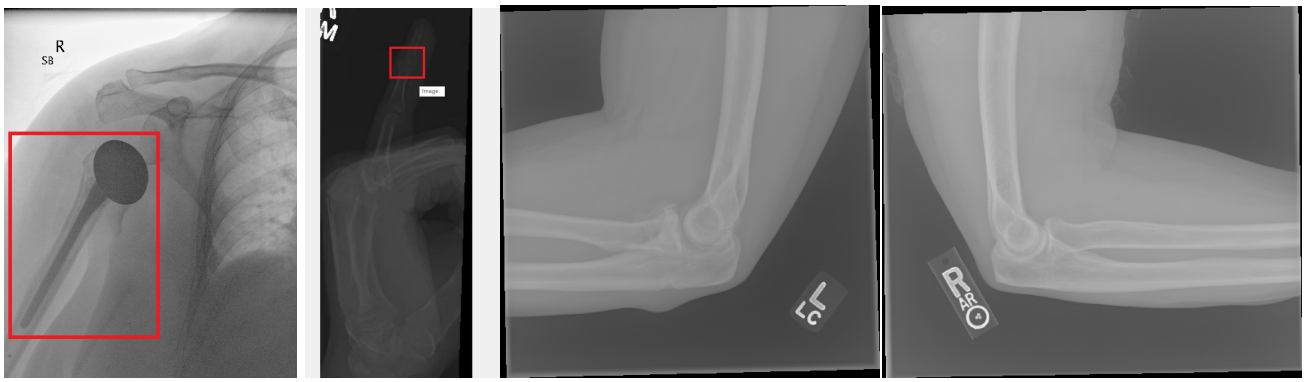

(a) (b) (c) (d)

FIGURE 1. Examples of musculoskeletal radiograph: (a) and (b) show that there are other interfering organ tissues in the complicated backgrounds. (c) and (d) show abnormal and normal elbows, respectively, but they are highly similar and difficult to distinguish.

However, the abnormal regions are small while other interfering organ tissues are redundant for diagnosis, and some abnormal and normal regions are relatively similar, leading to confusion in musculoskeletal abnormality diagnosis. Inspired by it, a Lesion-guided Recurrent Feature Sampling (LRFS) module is devised to locate the musculoskeletal abnormality regions from radiographs, consisting of musculoskeletal regions segmentation, musculoskeletal feature extractor, and recurrent sampling strategy, as shown in Lesion-guided Recurrent Feature Sampling Module of Fig. 2, which are described as follows:

1) Musculoskeletal Regions Segmentation

Precise musculoskeletal region segmentation results in abundant and reliable node feature information for musculoskeletal graph construction. Here, a high-performance medical image segmentation network, namely Swin-UNet [26], is used to accurately depict the boundaries of the bones. Swin-UNet is a semantic segmentation method that integrates residual skip-connection and Transformer attention mechanism to aggregate musculoskeletal regions, and especially it can focus on skeletal abnormal areas for superior performance.

2) Musculoskeletal Feature Extractor

The musculoskeletal regions segmented by Swin-UNet are used to excavate normality or abnormality information in bone morphology to strengthen the diagnostic capability of the proposed approach for clinical bone abnormality detection. Specifically, the feature maps generated from the Swin-Unet are used as the predictive node features in musculoskeletal radiographs. Therefore, different bone descriptors are presented as follows: finger degeneration; operative plate in the forearm; screw fixation in the humerus; shoulder fractures; external fixation in the wrist, as shown in Fig. 3.

3) Recurrent Sampling Strategy

The node matrix which contains representative feature vectors plays a significant role in the performance of the model in the graph convolutional network. However, features exacted by specific methods are routinely redundant or insufficient. In order to restrain such problems, a recurrent sampling strategy is proposed to obtain the most representative features from the feature exaction tools. Specifically, let matrix $M \epsilon R^{nxm}$ denotes the feature optimization matrix realized by a convolution operation. Then the node feature matrix H^j is calculated by the formula:

$$H^j_{kxm} = H^j_{kxn} M^j_{nxm} \tag{1}$$

where H^j_{kxm} denotes the optimized matrix $H \epsilon R^{kxm}$ in the j-th epoch.

B. ADAPTIVE GRAPHSAGE ATTENTION MODULE FOR MUSCULOSKELETAL ABNORMALITY DIAGNOSIS

Another challenging factor for musculoskeletal abnormality detection is that the convolutional neural networks play poor performance in modeling the abnormal dependencies between different musculoskeletal radiographs, including the finger, humerus, elbow, forearm, hand, shoulder, and wrist. Meanwhile, the graph convolutional neural network has been proven to be an effective tool for information modeling between different-type data. Moreover, constructing an intrinsic relation graph that reveals interactions between bones is critical for bone abnormality detection, where each musculoskeletal predictive feature maps form the nodes of the smallest adjacent graph and edges denote the images are all adjacent to each other. Motivated by these observations, the Adaptive Graphsage Attention (AGA) module is designed to diagnose bone abnormality in the abnormal bone regions, where the adaptive graph attention module can aggregate the information between adjacent nodes instead of learning the attention weights in every node, as shown in Fig. 2. Next, the general graph convolutional network is described, and then the Adaptive Graphsage Attention (AGA) Module is presented as follows.

1) Graph Convolutional Network

The graph convolutional network (GCN) is routinely used to research irregular data structures in non-Euclidean space,

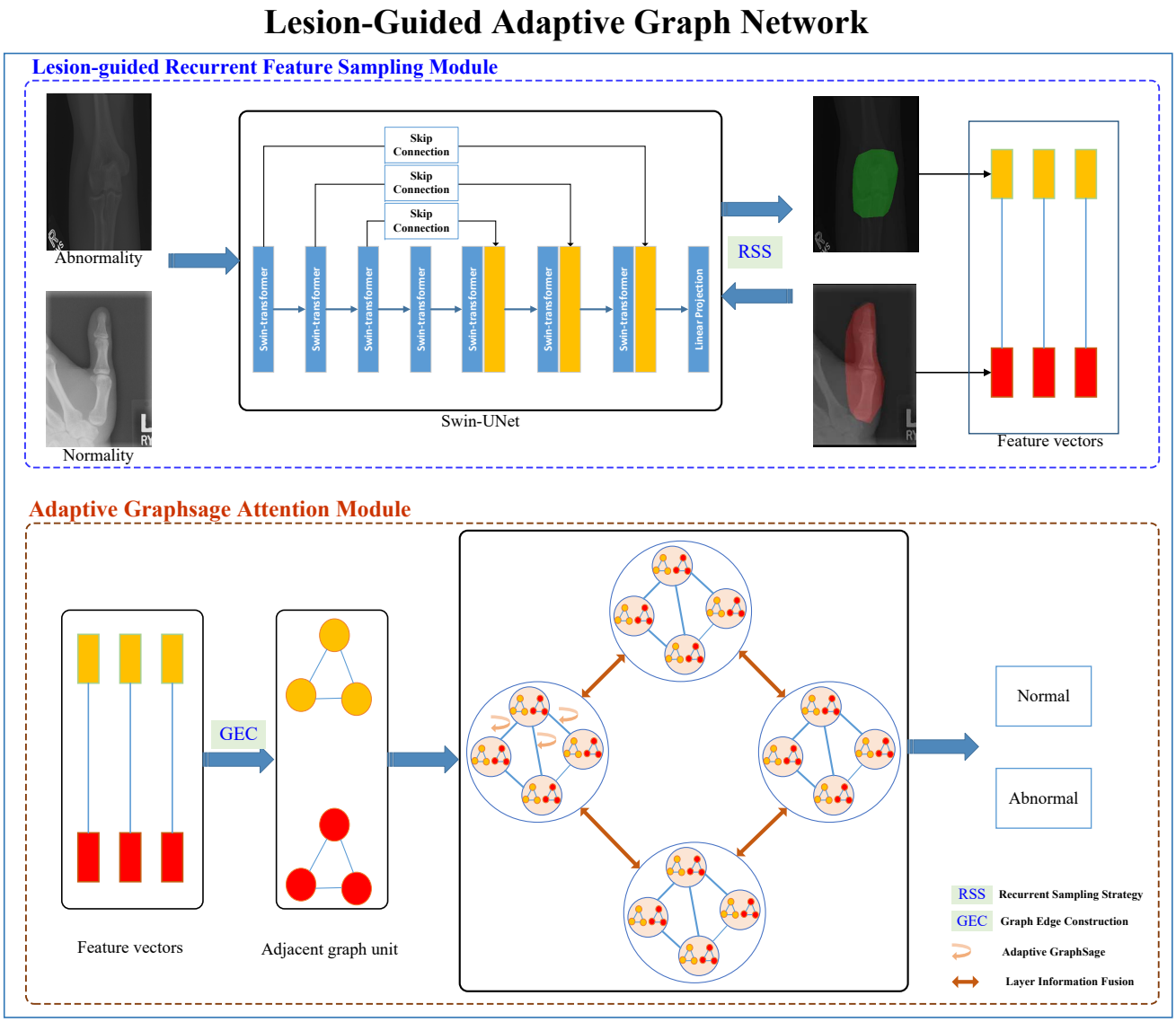

FIGURE 2. Architecture of the proposed Lesion-Guided Adaptive Graph Network (LGAG-Net), where the Lesion-guided Recurrent Feature Sampling (LRFS) module is first devised to segment the corresponding musculoskeletal abnormality regions, and then the Adaptive Graphsage Attention (AGA) module is designed to carry out the bone abnormality detection.

such as knowledge graph [27], traffic forecasting [28], recommender system [29], computer vision [30] [31]. A graph involved node feature X can be defined as

$$G = (V, E, X), \tag{2}$$

where $X \epsilon R^{nxd}$ contains n d-dimensional feature vectors, V denotes the node set and E presents the edge set. An adjacency matrix $A \epsilon R^{nxn}$ is generated based on the edge set E. Let $H^l = \{h_1, h_2, \ldots, h_k\}$, $h_i \epsilon R^n$ represents the input node features matrix of the l-th layer, where k is the number of nodes, and n is the number of features in each node, the typical implementation of graph convolution network [32] is expressed as follows:

$$H^{l+1} = \sigma(\tilde{D}^{-\frac{1}{2}}\tilde{A}\tilde{D}^{-\frac{1}{2}}H^l W^l) \tag{3}$$

where $\tilde{A} = A + I$, $\tilde{D}_{ii} = \Sigma_j \tilde{A}_{ij}$ is the normalized degree matrix, W^l is the weights in the l-th layer, and σ is the activation function, where the ReLU is used in our experiments.

C. ADAPTIVE GRAPHSAGE ATTENTION MODULE

1) Musculoskeletal Graph Edge Construction

In the complicated bone graph, the potential interaction relationship between graph nodes is established based on human unit S_H. Firstly, we construct the smallest adjacent graph unit S_A in which the adjacency matrix A_S is generated according to that all the images in the same file are adjacent to each other. Secondly, a node feature vector in human unit S_H is calculated from the weighted average of all node features in the S_A, and the node adjacency matrix A_H is produced by calculating the category between the output feature maps from the Swin-

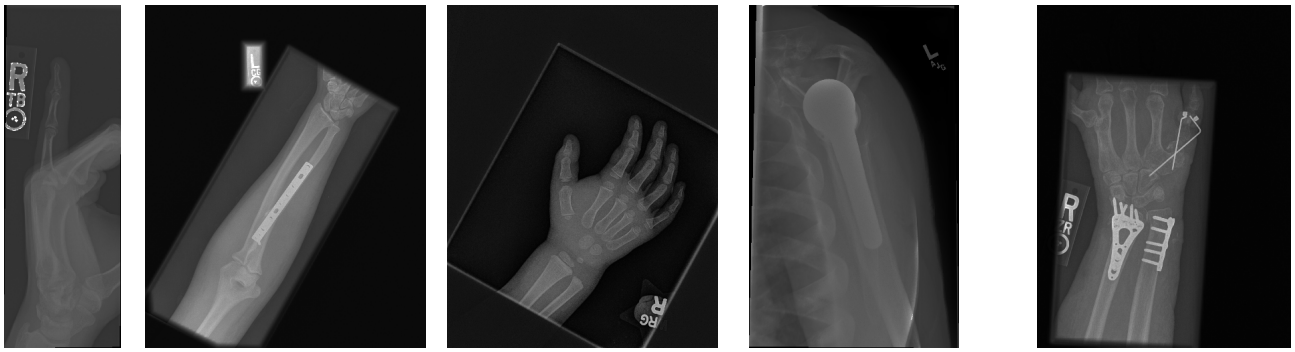

(a) (b) (c) (d) (e)

FIGURE 3. Abnormality bones. (a) An abnormal finger with degenerative changes. (b) An abnormal forearm with the operative plate. (c) The screw fixation of the humerus (d) Shoulder fractures (e) External fixation in wrist.

Unet.

2) Adaptive GraphSage

Representative feature vectors and edge relationships are absolutely vital for subsequent information aggregation in graph convolution networks, and various graph convolution networks can be applied to establish adjacent graphs based on node feature and edge information. In [32], it can learn the graph information through aggregation functions in Eq. 3 and combines the neighbor's node feature and the information captured from other adjacent nodes. However, this graph-constructing strategy cannot automatically assign appropriate weights for features according to the relationship between adjacent nodes. In other words, the information from its k-hop neighbor nodes is aggregated into the node through the connecting edges, which is unreasonable for the bone graph because of the redundancy in the node feature.

Inspired by [33], an Adaptive Graphsage Attention (AGA) module is proposed to learn the self-attention weights W between all the adjacent node features. The learnable linear transformation in l-layer form 3 can be expressed as follows:

$$H^l = \tilde{D}^{-\frac{1}{2}}\tilde{A}\tilde{D}^{-\frac{1}{2}}H^l \tag{4}$$

Instead of learning the self-attention weights in every node, we tend to aggregate the information of features just between adjacent nodes. We perform the self-attention on the nodes using a shared attentional coefficient matrix W by computing attention coefficients:

$$w_{i,j} = f(h_i, h_j) \tag{5}$$

where $w_{i,j}$ presents the interaction relationship degree of node j's features to node i, $f(\cdot)$ denotes the convolution operation based on node features H. As the $\tilde{D}$ is the normalized degree matrix, the self-attention coefficients between adjacent nodes can be expressed as

$$W_A = \tilde{D}^{-\frac{1}{2}}\tilde{A}\tilde{D}^{-\frac{1}{2}} \cdot W \tag{6}$$

where $\cdot$ means the dot multiplication in the matrix. The softmax function is used to convert the W_A matrix into $\tilde{W}_A$ by normalizing the row coefficients:

$$w_j = \frac{exp(w_j)}{\sum_i exp(w_{ij})} \tag{7}$$

where w_j denotes the j column coefficients in i-th row, and then the k-layer transform is presented as:

$$H^l = \tilde{W}^l H^l \tag{8}$$

Finally, the perfect formula can be described as:

$$H^l = \tilde{W}_S^l \tilde{W}_H^l \tilde{W}_E^l H^l \tag{9}$$

where $\tilde{W}_S^l$ denotes the deformable matrix of smallest adjacent graph, $\tilde{W}_H^l$ presents the deformable matrix of human unit, $\tilde{W}_E^l$ denotes the deformable matrix of node features.

3) Layer Information Fusion

The adaptive graph attention network is formed by stacking multi-layer structures, and there exists information loss in forwarding propagation. As reported by [34] that identity mappings in residual networks are able to improve the generalization of models, a residual attention module is proposed to deal with the problem of information loss, and it can be expressed as follows:

$$x^{l+1} = wx^l + f(x^l) \tag{10}$$

where w denotes the self-attention coefficients, $f(\cdot)$ presents convolution operation, x^l presents the input of l-layer.

III. EXPERIMENTS AND RESULTS ANALYSIS

A. DATASET AND EVALUATION METRICS

The proposed approach is evaluated on the MURA dataset [35], which consists of 14656 images taken from seven different types of extreme musculoskeletal radiographs, as recorded in Table 1. In this experiment, the dataset is split into three folds for cross-validation, including 10259 training images, 2932 validation images, and 1465 test images.

To verify the effectiveness of the proposed LGAG-Net, Cohen's kappa statistic is used to compare the results tested on seven type of bone radiographs. Accuracy, recall, precision, and F-score are used as evaluation metrics in comprehensive comparison between typical networks, and they are defined as:

$$Accuracy = \frac{TP + TN}{TP + TN + FP + FN}, \tag{11}$$

$$Precision = \frac{TP}{TP + FP}, \tag{12}$$

$$Recall = \frac{TP}{TP + FN}, \tag{13}$$

and

$$\text{F1-score} = 2 \times \frac{Precision \times Recall}{Precision + Recall}, \tag{14}$$

where TP is the correctly classified abnormal bones, FP is the wrongly predicted abnormal bones, FN is the correctly classified normal bones, and FN is the wrongly predicted normal bones. In addition, the kappa statistic score can be defined as:

$$Kappa = \frac{Accuracy - CAccuracy}{1 - CAccuracy}, \tag{15}$$

where CAccuracy denotes the class accuracy, computed by

$$CAccuracy = \frac{\sum_{i=1}^{N} a_i b_i}{N^2}, \tag{16}$$

in which a_i is the actual number of samples for each category, and b_i is the number of samples predicted for each class.

B. IMPLEMENTATION DETAILS

The AMFA-Net is constructed by Pytorch 1.6.0 [36] on a workstation with four NVIDIA GeForce GTX 1080Ti GPUs. The Adam optimizer is initialized with a learning rate of $1e^{-3}$, and the CrossEntropy is regarded as the loss function. To prevent over-fitting, dropout is set to 0.2 during training and all models are trained for 100 epochs with a batch size of 8. Moreover, all the node features are normalized by subtracting the mean and dividing by its standard deviation channel-wise.

C. EXPERIMENTAL RESULTS

1) Comparison with State-of-the-Art

To prove the effectiveness of the proposed LGAG-Net, several recent state-of-the-art methods are used for bone abnormality detection, including MURA [35], CapsNet [1], and MSCNN-GCN [25], and some classical deep learning models, which are described as follows:

First, MURA [35] is a baseline model to detect and localize abnormalities in deep learning, which takes as input one or more views for the model. For the CapsNet [1] method, it has shown promising features for musculoskeletal radiographs abnormality detection with 10% higher kappa score than Densenet169. Besides, the MSCNN-GCN, consisting of a multi-scale convolution neural network (MSCNN) with fully connected graph convolution network (GCN), achieves top scores on both F1-score and kappa metric for the detection of musculoskeletal abnormalities. Finally, some deep learning-based networks are used, i.e., VGG19 [37], ResNet50 [38], DenseNet161 [41], EfficientNet-b7 [40], MobileNetV2 [39] are leveraged to train for comparative experiments. This MURA dataset is split in the same way as [25] and the recorded results from the paper are utilized for comparison, and the experimental results are given in Table 2 and 3. From Table 2 that we can see that the proposed LGAG-Net is able to achieve the best outcomes, achieving the kappa score of 0.836, 0.862, 0.812, 0.857, 0.884, 0.876, 0.957, on finger, humerus, elbow, forearm, hand, shoulder, and wrist, respectively. Besides, the average kappa score can be up to 0.869, which is better than other methods. These excellent performance demonstrate the proposed can be used as an effective tool for bone abnormality detection from musculoskeletal radiograph. Furthermore, the LGAG-Net can achieve advancements of 3.3% on the kappa score, compared to the second best MSCNN-GCN methods, validating that the proposed LGAG-Net show higher anti-interference ability to diagnose musculoskeletal abnormality based on graph convolution network (GCN). Finally, five classical deep learning networks, i.e., VGG19 [37], ResNet50 [38], DenseNet161 [41], EfficientNet-b7 [40], MobileNetV2 [39] are tested on the MURA dataset, and the results are listed in Table 3. It can be found that the proposed LGAG-Net outperforms other models, achieving the best performance of 87.81%, 91.73%, 86.67%, 89.13% and 86.84% on Accuracy, Precision, Recall, F1-score, and Cohen âĂŹs kappa, respectively, achieving significant improvements for VGG19 [37], ResNet50 [38], EfficientNet-b7 [40], MobileNetV2 [39], demonstrating that the proposed LGAG-Net is a feasible approach for bone abnormality detection.

D. ABLATION STUDIES

1) Recurrent sampling strategy

A recurrent sampling strategy is proposed to deal with the problem of redundancy or insufficiency in features exacted by deep learning models. Compared with general features exaction methods, such as ResNet50, the recurrent sampling strategy is able to screen valuable information by convolution operation matrix. Comparative results are recorded in Table 4, it can be inferred that the proposed method achieves state-of-the-art performance on accuracy and Cohen's kappa score.

2) Adaptive GraphSage

As illustrated in Section 3.3, in order to assign appropriate weights for information aggregation between node features, we propose a self-attention mechanism on the adjacent node. Experiments of using different graph edge configuration methods are shown in Table 4, where GC and AGC denote graph convolution and adaptive graph convolution method respectively. Compared with the result from GC in the first row, utilizing AGC achieves improvements from 82.7% to 84.8% for the patch accuracy, as well as the Cohen's kappa

TABLE 1. The characteristics of the training and validation sets for the MURA dataset [35]

Study	Train		Validation		Total
	Normal	Abnormal	Normal	Abnormal	
Elbow	1,094	660	92	66	1,912
Finger	1,280	655	92	83	2,110
Hand	1,497	521	101	66	2,185
Humerus	321	271	68	67	727
Forearm	590	287	69	64	1,010
Shoulder	1,364	1,457	99	95	3,015
Wrist	2,134	1,326	140	97	3,697
Total	8,280	5,177	661	538	14,656

TABLE 2. Kappa statistic score obtained by MURA method, CapsNet, MSCNN-GCN and LGAG-Net

Image	MURA [35] (95% CI)	CapsNet [1] (95% CI)	MSCNN-GCN [25] (95% CI)	LGAG-Net (95% CI)
Finger	0.389 (0.446, 0.332)	0.735 (0.959, 0.512)	0.744 (0.806, 0.682)	**0.836** (0.826, 0.846)
Humerus	0.600 (0.642, 0.558)	0.754 (0.896, 0.612)	0.843 (0.936, 0.749)	**0.862** (0.851, 0.873)
Elbow	0.710 (0.745, 0.674)	0.733 (0.754, 0.713)	0.774 (0.831, 0.717)	**0.812** (0.801, 0.823)
Forearm	0.737 (0.766, 0.707)	0.785 (0.795, 0.775)	0.837 (0.912, 0.762)	**0.857** (0.837, 0.877)
Hand	0.851 (0.871, 0.830)	0.835 (0.856, 0.881)	0.855 (0.897, 0.814)	**0.884** (0.872, 0.886)
Shoulder	0.729 (0.760, 0.697)	0.856 (0.876, 0.836)	0.862 (1.000, 0.678)	**0.876** (0.856, 0.896)
Wrist	0.931 (0.940, 0.922)	0.908 (0.917, 0.898)	0.936 (0.948, 0.924)	**0.957** (0.943, 0.971)
Average	0.705 (0.700, 0.710)	0.801 (0.865, 0.738)	0.836 (0.911, 0.761)	**0.869** (0.855, 0.881)

TABLE 3. Performance comparison of CNN models trained on the MURA dataset

Model	Accuracy (%)	Precision (%)	Recall (%)	F1-score (%)	Cohen's kappa (%)
VGG19 [37]	81.95	82.70	81.61	81.71	63.61 (62.79, 64.43)
ResNet50 [38]	81.64	82.40	81.29	81.39	62.98 (62.15, 63.80)
MobileNetV2 [39]	81.95	82.84	81.58	81.68	63.59 (62.77, 64.41)
EfficientNet-b7 [40]	81.86	82.09	81.65	81.73	63.52 (62.70, 64.34)
DenseNet161 [41]	83.27	83.52	83.06	83.15	66.35 (65.56, 67.14)
LGAG-Net	**87.81**	**91.73**	**86.67**	**89.13**	**86.84 (85.51, 88.17)**

score from 83.1% to 85.2% because the self-attention module can assimilate effective information from adjacent nodes. In addition, the accuracy is further improved with 1.1% using the proposed graph edge configuration while node features are obtained from the recurrent sampling strategy. This is because it guarantees that the valuable feature information from the adjacent node can be transmitted to the local node.

3) Layer information fusion

A residual network [38] is proposed to deal with the notorious problem of vanishing/exploding gradients, that is, there exists information loss in forwarding propagation. Inspired by it, a residual attention module is embedded into the network structure layers and the comparative experimental results are recorded in Table 4. Graph convolution network embedded with residual attention module achieves the highest results, 87.8% for classification accuracy and 86.84% for Cohen's kappa score, which demonstrates the residual attention module is an informative tool for capturing the corresponding contextual information in bone abnormality regions.

IV. CONCLUSIONS

In this paper, a Lesion-Guided Adaptive Graph Network (LGAG-Net) is proposed for bone abnormality detection from musculoskeletal radiograph, where the lesion-guided recurrent feature sampling module is first designed to localize the corresponding musculoskeletal abnormality regions, and then the adaptive graphsage attention module is developed to perform bone abnormality detection on the located musculoskeletal abnormality regions. Experiments on the MURA dataset show that the proposed LGAG-Net can achieve the best performance on bone abnormality detection, further maintaining musculoskeletal health and preventing complications requires encouragement of physical activities to promote physical fitness and normal neuromuscular development.

REFERENCES

[1] A. Saif, C. Shahnaz, W.-P. Zhu, and M. O. Ahmad, "Abnormality detection in musculoskeletal radiographs using capsule network," *IEEE Access*, vol. 7, pp. 81 494–81 503, 2019.

[2] Y. K. Tamilselvam, J. Ganguly, R. V. Patel, and M. Jog, "Musculoskeletal

TABLE 4. Average accuracy and Cohen's kappa score on the MURA dataset, where RSS denotes recurrent sampling strategy. GEC represents the graph edge configuration method, where GC and AGC denote graph convolution and adaptive graph convolution respectively. IP represents information propagation, whereas DIP and LIF denote direct information propagation and layer information fusion propagation, respectively

Node Features	GEC	IP	Accuracy	Cohen's kappa (%)
Feature vector	GC	DIP	82.7±1.21	83.1±1.32
Feature vector	AGC	DIP	84.8±1.92	85.2±1.62
Feature vector	AGC	LIF	85.7±2.11	85.8±1.38
Feature vector & RSS	GC	DIP	84.3±2.02	84.9±2.41
Feature vector & RSS	AGC	DIP	85.4±0.93	85.6±2.09
Feature vector & RSS	AGC	LIF	**87.8±2.03**	**86.9±1.33**

model to predict muscle activity during upper limb movement," *IEEE Access*, vol. 9, pp. 111 472–111 485, 2021.

[3] J. Van Mulders, S. Goossens, L. Monteyne, L. De Strycker, and L. Van Der Perre, "Contactless multi-sensor solution for e-treatment of musculoskeletal disorders," *IEEE Access*, vol. 9, pp. 20 368–20 375, 2021.

[4] B. Vellas, D. Scrase, G. Rosenberg, S. Andrieu, I. A. de Carvalho, and L. Middleton, "Who guidelines on community-level interventions to manage declines in intrinsic capacity: The road to prevention cognitive decline in older age?" 2018.

[5] E. Sebbag, R. Felten, F. Sagez, J. Sibilia, H. Devilliers, and L. Arnaud, "The world-wide burden of musculoskeletal diseases: A systematic analysis of the world health organization burden of diseases database," *Annals of the Rheumatic Diseases*, vol. 78, no. 6, pp. 844–848, 2019.

[6] United States Bone and Joint Initiative, "The burden of musculoskeletal diseases in the United States (BMUS)," Available online: http://www.boneandjointburden.org, 2019, (accessed on 14 June 2019).

[7] M. Zhou, H. Wang, X. Zeng, P. Yin, J. Zhu, W. Chen, X. Li, L. Wang, L. Wang, Y. Liu *et al.*, "Mortality, morbidity, and risk factors in china and its provinces, 1990–2017: A systematic analysis for the global burden of disease study 2017," *The Lancet*, vol. 394, no. 10204, pp. 1145–1158, 2019.

[8] S. L. James, D. Abate, K. H. Abate, S. M. Abay, C. Abbafati, N. Abbasi, H. Abbastabar, F. Abd-Allah, J. Abdela, A. Abdelalim *et al.*, "Global, regional, and national incidence, prevalence, and years lived with disability for 354 diseases and injuries for 195 countries and territories, 1990–2017: a systematic analysis for the global burden of disease study 2017," *The Lancet*, vol. 392, no. 10159, pp. 1789–1858, 2018.

[9] R. J. McDonald, K. M. Schwartz, L. J. Eckel, F. E. Diehn, C. H. Hunt, B. J. Bartholmai, B. J. Erickson, and D. F. Kallmes, "The effects of changes in utilization and technological advancements of cross-sectional imaging on radiologist workload," *Academic Radiology*, vol. 22, no. 9, pp. 1191–1198, 2015.

[10] J. Davidson, A. M. N. dos Santos, K. M. B. Garcia, C. Y. Liu, P. C. João, M. H. Miyoshi, and A. L. Goulart, "Photogrammetry: An accurate and reliable tool to detect thoracic musculoskeletal abnormalities in preterm infants," *Physiotherapy*, vol. 98, no. 3, pp. 243–249, 2012.

[11] E. Paschalis, S. Gamsjaeger, and K. Klaushofer, "Vibrational spectroscopic techniques to assess bone quality," *Osteoporosis International*, vol. 28, no. 8, pp. 2275–2291, 2017.

[12] M. O. Chan, E. S. Sen, E. Hardy, P. Hensman, E. Wraith, S. Jones, T. Rapley, and H. E. Foster, "Assessment of musculoskeletal abnormalities in children with mucopolysaccharidoses using pgals," *Pediatric Rheumatology*, vol. 12, no. 1, pp. 1–9, 2014.

[13] I. Hmeidi, M. Al-Ayyoub, H. Rababah, and Z. Khatatbeh, "Detecting hand bone fractures in X-Ray images," in *Proceedings of the World Congress on Multimedia and Computer Science*, 2013.

[14] S. F. Kurniawan, I. DARMA PUTRA, and A. K. O. Sudana, "Bone frature detection using opencv." *Journal of Theoretical and Applied Information Technology*, vol. 64, no. 1, 2014.

[15] N. Johari and N. Singh, "Bone fracture detection using edge detection technique," in *Soft Computing: Theories and Applications*. Springer, 2018, pp. 11–19.

[16] S. Omar, A. Ngadi, and H. H. Jebur, "Machine learning techniques for anomaly detection: An overview," *International Journal of Computer Applications*, vol. 79, no. 2, 2013.

[17] G. Cho, J. Yim, Y. Choi, J. Ko, and S.-H. Lee, "Review of machine learning algorithms for diagnosing mental illness," *Psychiatry Investigation*, vol. 16, no. 4, p. 262, 2019.

[18] P. K. Mall, P. K. Singh, and D. Yadav, "Glcm based feature extraction and medical x-ray image classification using machine learning techniques," in *Proceedings of the IEEE Conference on Information and Communication Technology*, 2019, pp. 1–6.

[19] B. Qamar, M. M. Jawaid, and M. A. Memon, "Computer assisted solution for bone anomaly detection in x-ray images," *ResearchGate*, pp. 1–6, 2021.

[20] G. Chada, "Machine learning models for abnormality detection in musculoskeletal radiographs," *Reports-Medical Cases, Images, and Videos*, vol. 2, no. 4, pp. 1–11, 2019.

[21] D. Banga and P. Waiganjo, "Abnormality detection in musculoskeletal radiographs with convolutional neural networks (ensembles) and performance optimization," *arXiv preprint arXiv:1908.02170*, 2019.

[22] M. Goyal, R. Malik, D. Kumar, S. Rathore, and R. Arora, "Musculoskeletal abnormality detection in medical imaging using gncnnr (group normalized convolutional neural networks with regularization)," *SN Computer Science*, vol. 1, no. 6, pp. 1–12, 2020.

[23] G. Mehr, "Automating abnormality detection in musculoskeletal radiographs through deep learning," *arXiv preprint arXiv:2010.12030*, 2020.

[24] R. M. Jones, A. Sharma, R. Hotchkiss, J. W. Sperling, J. Hamburger, C. Ledig, R. OToole, M. Gardner, S. Venkatesh, M. M. Roberts *et al.*, "Assessment of a deep-learning system for fracture detection in musculoskeletal radiographs," *NPJ Digital Medicine*, vol. 3, no. 1, pp. 1–6, 2020.

[25] S. Liang and Y. Gu, "Towards robust and accurate detection of abnormalities in musculoskeletal radiographs with a multi-network model," *Sensors*, vol. 20, no. 11, p. 3153, 2020.

[26] H. Cao, Y. Wang, J. Chen, D. Jiang, X. Zhang, Q. Tian, and M. Wang, "Swin-unet: Unet-like pure transformer for medical image segmentation," in *Proceedings of European Conference on Computer Vision (ECCV)*, 2022, pp. 205–218.

[27] M. Schlichtkrull, T. N. Kipf, P. Bloem, R. Van Den Berg, I. Titov, and M. Welling, "Modeling relational data with graph convolutional networks," in *European Semantic Web Conference*, 2018, pp. 593–607.

[28] Z. Cui, K. Henrickson, R. Ke, and Y. Wang, "Traffic graph convolutional recurrent neural network: A deep learning framework for network-scale traffic learning and forecasting," *IEEE Transactions on Intelligent Transportation Systems*, vol. 21, no. 11, pp. 4883–4894, 2019.

[29] H. Wang, F. Zhang, J. Wang, M. Zhao, W. Li, X. Xie, and M. Guo, "Exploring high-order user preference on the knowledge graph for recommender systems," *ACM Transactions on Information Systems (TOIS)*, vol. 37, no. 3, pp. 1–26, 2019.

[30] C.-W. Lee, W. Fang, C.-K. Yeh, and Y.-C. F. Wang, "Multi-label zero-shot learning with structured knowledge graphs," in *Proceedings of the IEEE Conference on Computer Vision and Pattern Recognition (CVPR)*, 2018, pp. 1576–1585.

[31] Y. Zhou, S. Graham, N. Alemi Koohbanani, M. Shaban, P.-A. Heng, and N. Rajpoot, "CGC-Net: Cell graph convolutional network for grading of colorectal cancer histology images," in *Proceeedings of the IEEE/CVF International Conference on Computer Vision (ICCV)*, 2019, pp. 1–11.

[32] T. N. Kipf and M. Welling, "Semi-supervised classification with graph convolutional networks," *arXiv preprint arXiv:1609.02907*, 2016.

[33] P. Veličković, G. Cucurull, A. Casanova, A. Romero, P. Lio, and Y. Bengio, "Graph attention networks," *arXiv preprint arXiv:1710.10903*, 2017.

[34] K. He, X. Zhang, S. Ren, and J. Sun, "Identity mappings in deep residual networks," in *Proceedings of the European Conference on Computer Vision (ECCV)*, 2016, pp. 630–645.

[35] P. Rajpurkar, J. Irvin, A. Bagul, D. Ding, T. Duan, H. Mehta, B. Yang, K. Zhu, D. Laird, R. L. Ball *et al.*, "MURA: Large dataset for abnormality detection in musculoskeletal radiographs," *arXiv preprint arXiv:1712.06957*, 2017.
[36] A. Paszke, S. Gross, F. Massa, A. Lerer, J. Bradbury, G. Chanan, T. Killeen, Z. Lin, N. Gimelshein, L. Antiga *et al.*, "Pytorch: An imperative style, high-performance deep learning library," in *Proceedings of the Advances in Neural Information Processing Systems (NIPS)*, 2019, pp. 8026–8037.
[37] K. Simonyan and A. Zisserman, "Very deep convolutional networks for large-scale image recognition," *arXiv preprint arXiv:1409.1556*, 2014.
[38] K. He, X. Zhang, S. Ren, and J. Sun, "Deep residual learning for image recognition," in *Proceedings of the IEEE Conference on Computer Vision and Pattern Recognition (CVPR)*, 2016, pp. 770–778.
[39] A. Howard, A. Zhmoginov, L.-C. Chen, M. Sandler, and M. Zhu, "Inverted residuals and linear bottlenecks: Mobile networks for classification, detection and segmentation," pp. 1–12, 2018.
[40] M. Tan and Q. Le, "Efficientnet: Rethinking model scaling for convolutional neural networks," in *Proceedings of the International Conference on Machine Learning Research (PMLR)*, 2019, pp. 6105–6114.
[41] G. Huang, Z. Liu, L. Van Der Maaten, and K. Q. Weinberger, "Densely connected convolutional networks," in *Proceedings of the IEEE Conference on Computer Vision and Pattern Recognition (CVPR)*, 2017, pp. 4700–4708.

YONG LIAO was born in Loudi, Hunan, P.R. China, in 1990. He received the PHD's degree from Guangdong University of Technology, P.R. China. Now, he is an assistant professor in the School of Physics, Electronics and Electrical Engineering, at Xiangnan University. His research interest includes intelligent manufacturing system design, optimal control theory, and object detection.

XIANG LI was born in ChenZhou, Hunan, P.R. China, in 1982. He received the PHD's degree from Guangdong University of Technology, P.R. China. Now, he is an Associate Professor, at the School of Physics, Electronics and Electrical Engineering, and deputy director of the academic affairs office, at Xiangnan University. The main research direction is computer-integrated manufacturing systems; System modeling, analysis and optimization; Control system simulation.

CHENGFENG PENG was born in Ganzhou, Jiangxi, P.R. China, in 1991. He received the PHD's degree from Guangdong University of Technology, P.R. China. Now, he is an assistant professor in the School of Physics, Electronics and Electrical Engineering, at Xiangnan University. His research interest includes intelligent manufacturing, job shop scheduling, optimal control theory, and image recognition.